Accurate and high-resolution measurements of UTLS water vapor by balloon-borne laser absorption spectroscopy

Simone Brunamonti[1], Yann Poltera[2,3], Gonzague Romanens[4], Alex Weitnauer[1], Philipp Scheidegger[1], Adrianos Filinis[2,3], Alistair Bell[2,3], Giovanni Martucci[4], Frank G. Wienhold[5], Thomas Peter[5], Peter Oelsner[6], Ruud Dirksen[6], Alexander Haefele[4], Lukas Emmenegger[1], Gunter Stober[2,3] and Béla Tuzson[1]

[1]Empa, Laboratory for Air Pollution/Environmental Technology, Dübendorf, Switzerland
[2]University of Bern, Institute of Applied Physics, Bern, Switzerland
[3]Oeschger Center for Climate Change Research, University of Bern, Bern, Switzerland
[4]Federal Office of Meterology and Climatology (MeteoSwiss), Payerne, Switzerland
[5]ETH Zürich, Institute for Atmospheric and Climate Science, Zürich, Switzerland
[6]Deutscher Wetterdienst/GRUAN Lead Center, Lindenberg, Germany

Correspondence to: Simone Brunamonti (simone.brunamonti@empa.ch) and Béla Tuzson (bela.tuzson@empa.ch)

Supplementary material

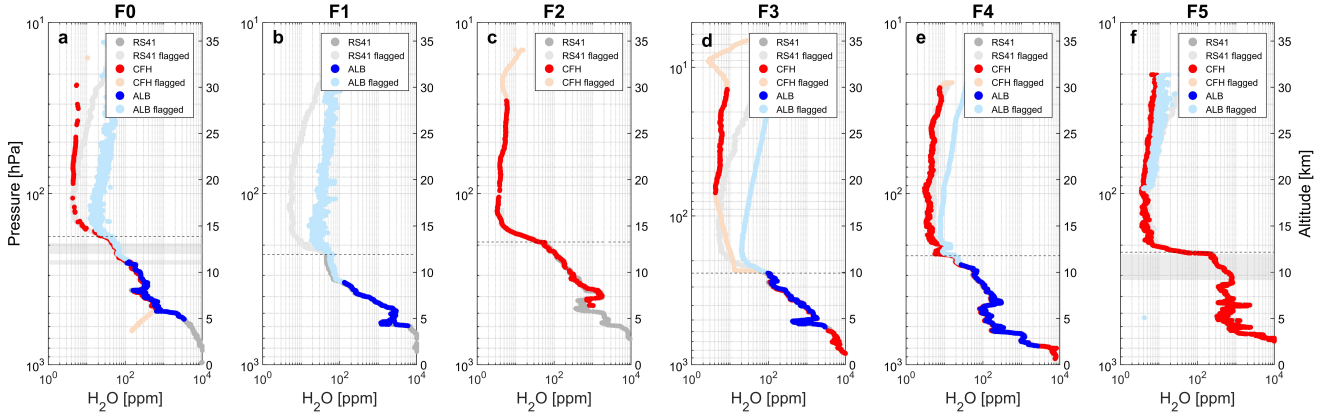

Figure S1. Vertical profiles of H_2O mixing ratio measured by ALBATROSS (blue), CFH (red) and RS41 (grey) during the descent of flights F0-F5 at 1 s resolution. Light-colored and dark-colored dots indicate flagged and valid measurement points, respectively. Black dashed lines indicate the tropopause level. Grey shadings in panels (a) and (f) indicate cirrus cloud layers, inferred from CFH ice saturation measurements.

S1. CFH data quality-check and flagging

All CFH profiles used in this work were individually quality-checked based on housekeeping data, and data points showing anomalous behaviour were flagged. This includes stratospheric measurements affected by contamination due to external moisture sources (see Section 2.2), data intervals affected by large instabilities of the mirror temperature controller (i.e., non-equilibrium errors: Poltera et al., 2026), and other technical failures (lack of R23 cryogen, low battery power).

Table S1 summarizes all CFH and ALBATROSS flagged intervals of the intercomparison and their corresponding rationale.

Flight	Instrument	Flagged interval	Reason for flagging
F0	ALBATROSS	$p < 200$ hPa (ascent), $p < 250$ hPa (descent)	Outside-cell absorption, In-cell contamination
	CFH	$p < 18$ hPa (ascent and descent)	External moisture sources
	CFH	$p > 470$ hPa (descent)	Lack of heating power (low battery power)
F1	ALBATROSS	$p < 330$ hPa (ascent and descent)	Outside-cell absorption (since ~60 hPa ascent), In-cell contamination
	CFH	$p < 19$ hPa (ascent and descent)	External moisture sources
F2	CFH	$p < 21$ hPa (ascent)	External moisture sources
	CFH	$p < 28$ hPa (descent)	Nonequilibrium errors
F3	ALBATROSS	10–15 hPa, 16–22 hPa, 24–47 hPa, 76–86 hPa, 122–135 hPa (ascent), $p < 242$ hPa (descent)	Outside-cell absorption (partly corrected by diffusion model: see Section S2)
	ALBATROSS	$p < 40$ hPa (ascent)	External moisture sources
	CFH	$p > 190$ hPa, 70–130 hPa (ascent), $p > 14$ hPa (descent)	Nonequilibrium errors (partly smoothed by moving average: see Section S1)
	CFH	$p < 10$ hPa (ascent)	External moisture sources
	CFH	70–235 hPa (descent)	Lack of cooling power (fully evaporated R23)
F4	ALBATROSS	$p < 275$ hPa (ascent), $p < 260$ hPa (descent)	Outside-cell absorption
	CFH	32–47 hPa (ascent), $p < 24$ hPa (descent)	Nonequilibrium errors
F5	ALBATROSS	$p < 82$ hPa (ascent)	External moisture sources
	CFH	116–224 hPa (ascent)	Nonequilibrium errors (partly replaced by descent data: see Section S1)
F6	ALBATROSS	$p < 40$ hPa (ascent), $p < 17$ hPa (descent)	External moisture sources
	CFH	$p < 32$ hPa (descent)	Nonequilibrium errors (replaced by ascent data)

Table S1. List of CFH and ALBATROSS flagged data intervals of all flights and their corresponding rationale.

For three of the CFH flagged intervals, which are particularly relevant for the comparison with ALBATROSS, the flagged data were replaced by either using information from the CFH descent profile (when available), or by applying a broad moving average to suppress controller instabilities. Namely, part of the flagged data in F3 were recovered by applying a ±75 s moving average in the troposphere (p > 190 hPa) and ±600 s in the lower stratosphere (~70–130 hPa) (see Fig. 3d). In F5, the flagged interval at ~110–220 hPa in ascent was replaced by descent data over the same pressure range, after applying a ±180 s moving average (Fig. 3f). Finally, the data affected by controller instabilities in the descent of F6 at p < 30 hPa were replaced by ascent data over the same pressure range (no moving average).

S2. ALBATROSS contamination modelling: flight F3

Figure S2 shows the ascent profiles of H_2O mixing ratio measured by ALBATROSS and CFH in the stratosphere during flight F3 (panel a), together with the purge gas flow rate of the ALBATROSS in-flight purging system (panel b) measured by the embedded flowmeter. The raw flowmeter data are converted to CO_2 flow rate using a calibration curve derived by laboratory measurements against a reference mass flow controller. The ALBATROSS raw retrieved H_2O mixing ratio is shown by light blue dots, whereas the corrected profile, as explained below, is shown by turquoise dots.

This flight was characterized by a discontinuous supply of the CO_2 purge gas by the ALBATROSS in-flight purging system, causing five contamination events in the retrieved H_2O mixing ratio in the stratosphere (grey shadings in Fig. S2). During these intervals, the H_2O mixing ratio shows a characteristic exponential increase with time, suggesting that this is due to the diffusion of moist air from the instrument's casing into the connector's volume, leading to outside-cell absorption (see Section 2.2).

Assuming that this process is governed by diffusion, here we discuss how the affected data can be (partially) modelled and corrected, by first estimating for each contaminated interval a linear baseline by interpolation, followed by the removal of an exponential contribution fitted to the residual signal. Further, we provide an independent consistency check of this approach using the water vapor mixing ratio inside the instrument enclosure (H_2O_{Box}) derived from housekeeping data of temperature and RH, showing that the exponential fit coefficients derived from the model functions are consistent with the H_2O_{Box} values measured by the internal RH sensor at different altitudes.

The increase in H_2O is described by Eq. S1, where t_0 is the onset of contamination (i.e., time when the flow rate stops), and a and b are exponential fit coefficients (in units of ppm and min, respectively). For each interval, Eq. S1 is fitted to the measured H_2O increase above the baseline level, defined as the linear interpolation of the H_2O mixing ratio in the last 10 s before the onset of contamination and the first 10 s after the end of it. Then, for each data point (i), the H_2O mixing ratio is corrected according to Eq. S2, using the baseline (H_2O_{BL}) and exponential correction term (y) of the corresponding interval.

Fig. S3 (panels a-b) illustrates the correction of the contaminated interval at 76–86 hPa (~18 km altitude), caused by a ~2 min gap in purge gas supply about 44 min after the launch of the balloon. Fig. S3a shows that the exponential function correctly reproduces the observed contamination trend with fit residuals within approximately ±0.2 ppm. The same procedure was applied to all the five contaminated intervals (grey shaded areas in Fig. S2) with similar results, although the observed behaviour

tends to deviate from an exponential increase on longer timescales (e.g., the 9 min interruption at ~15 hPa), where other factors likely play a role (e.g., small changes in flow rate near zero: see Fig. S2 at ~15 hPa; sensitivity of flowmeter response at low temperatures). Therefore, these intervals were excluded from the corrected profile.

From the assumption of a diffusion process it follows that, at the equilibrium state (i.e., when the connectors are completely filled with air from the enclosure), the measured H_2O mixing ratio is equal to the sum of the mixing ratio in the cell and H_2O_{Box}, scaled by the appropriate ratio in OPL. Therefore, the asymptotic value of $y(t)$, i.e., coefficient a, can be related to H_2O_{Box} by Eq. S3, through the ratio of the outside-cell OPL (OPL_{Out}) to the total OPL (OPL_{Cell} + OPL_{Out}).

$$y(t) = a\exp(-\frac{b}{t-t_0}) \quad [S1]$$

$$H_2O_{Corr,i} = H_2O_{Raw,i} - y(t_i) + H_2O_{BL}(t_i) \quad [S2]$$

$$H_2O_{Box} = \frac{OPL_{Cell} + OPL_{Out}}{OPL_{Out}}\, a \quad [S3]$$

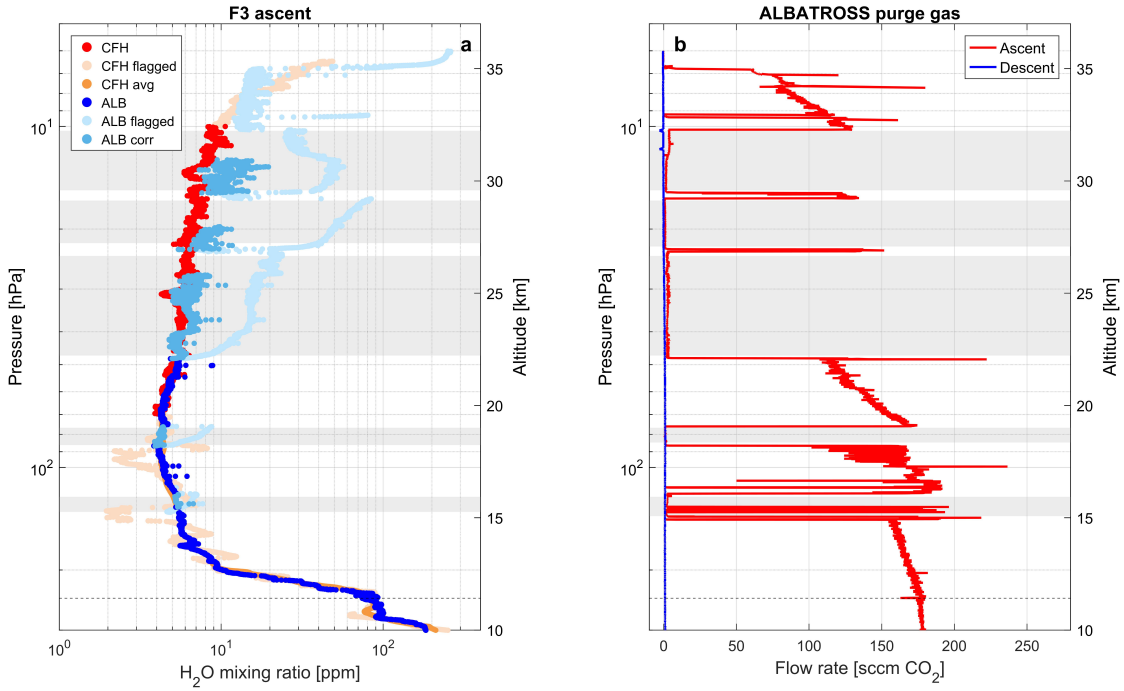

Figure S2. Panel (a): vertical profiles of H_2O mixing ratio measured by ALBATROSS (valid data: blue, flagged data: light blue, corrected data: turquoise) and CFH (valid data: red, flagged data: light red, corrected data: orange) during the ascent of flight F3 in the stratosphere (5–250 hPa pressure, ~10–36 km altitude). Panel (b): CO_2 flow rate of the ALBATROSS in-flight purging system measured by the embedded flowmeter during ascent (red) and descent (blue) of F3 in the stratosphere. Grey shaded areas indicate the five intervals of contaminated ALBATROSS measurements.

Fig. S3 (panels c-d) illustrates the H_2O_{Box} calculation and comparison with the exponential fit results. First, H_2O_{Box} is calculated from the temperature (T_{Box}), pressure and RH profiles measured by the MS8607 sensor embedded in the ALBATROSS's enclosure (see Section 2), using the Hardy (1998) parameterization for saturation vapor pressure over liquid water. The raw RH data from this sensor are calibrated based on laboratory measurements against a high accuracy HMP110 humidity sensor (Vaisala, Finland). The uncertainty on the RH measurements derived from this calibration is about ±2.5 % RH. Fig. S3c shows that $T_{Box} \approx -10$ °C throughout the ascent in the stratosphere (with an outside air temperature of about –65°C), while RH in the box increases with altitude in the stratosphere, up to ~20 % RH at 30 km altitude (10 hPa). The corresponding H_2O_{Box} profile (Fig. S3d) shows a substantial increase in the stratosphere, from ~2000 ppm at the tropopause to ~5×10^4 ppm (i.e., 5 % H_2O) at 30 km altitude. As discussed in Section 2.2, this high amount of internal moisture represents the main source of contamination for the ALBATROSS stratospheric retrievals.

The red dots in Fig. S3d are the values of H_2O_{Box} calculated according to Eq. S3 from the coefficient a of each of the contaminated intervals. The uncertainty bars on these dots correspond to different estimates of OPL_{Out}. As described in Section 2.2, two connectors are implemented in ALBATROSS, sealing the SC-MPC to the laser housing and to the detector, with lengths of about 16 mm and 9 mm, respectively. Since the leak tightness of the two connectors is presumably not the same, the measurement will reflect an average air diffusion flux for the two connectors. Therefore, H_2O_{Box} is calculated for three scenarios, corresponding to the limit cases: $OPL_{Out} = 16$ mm (i.e., diffusion only through the laser-side connector), $OPL_{Out} = 9$ mm (diffusion only through the detector-side connector), and $OPL_{Out} = 25$ mm (diffusion through both connectors). In all cases, $OPL_{Cell} = 6107$ mm, therefore the ratio in Eq. S3 varies between 1.0014–1.0041.

Fig. S3d shows that the results obtained from the fit coefficients are generally consistent with the H_2O_{Box} values derived by the internal RH sensor, and correctly reproduce the observed increase in H_2O mixing ratio in the box with altitude. This is true for all intervals except the highest contamination level at ~15 hPa, where other instrumental artifacts may play a role, such as the sensitivity of the MS8607 sensor at low temperatures and pressures. The good agreement between the two estimates of H_2O_{Box} provides a valuable and independent validation of this modelling approach, lending a high degree of confidence to the physical interpretation of the contamination mechanism, and hence to the corrected ALBATROSS profile shown in Fig. 6a.

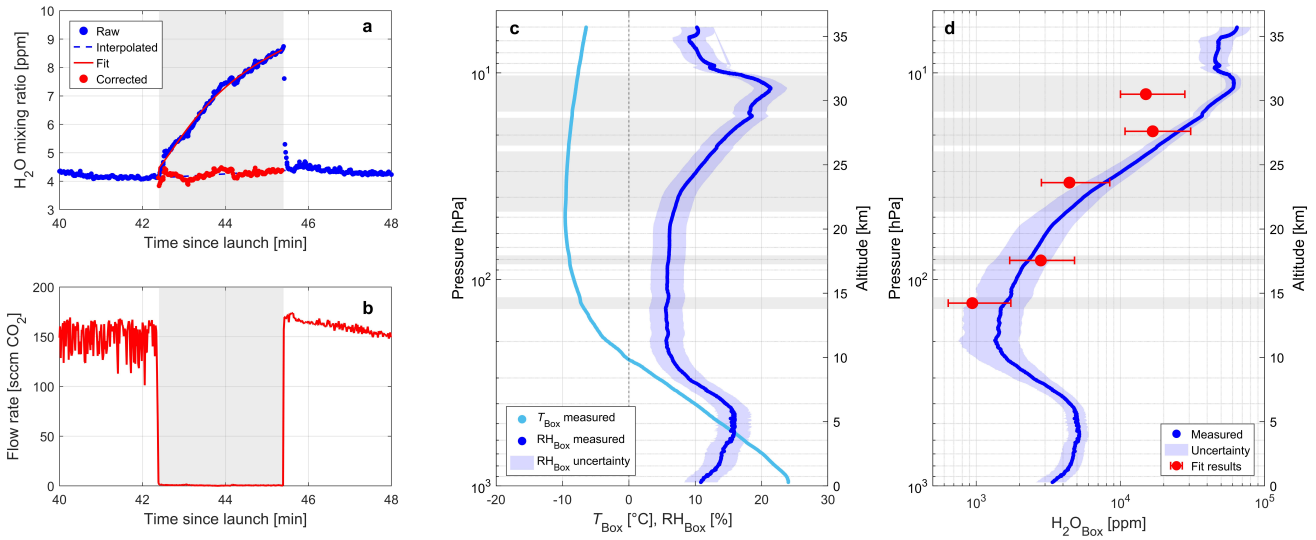

Figure S3. Panels (a-b) application of the correction procedure to the contaminated interval at 76–86 hPa pressure (~18 km altitude) in flight F3. Panel (a): timeseries of the raw H_2O mixing ratio from ALBATROSS (blue dots), the baseline H_2O mixing ratio (H_2O_{BL}, blue dashed line), the fitted H_2O mixing ratio (red line), and the corrected H_2O mixing ratio profile (red dots). Panel (b): time series of CO_2 flow rate measured by the flowmeter. The grey shaded area in panels (a-b) indicate the time interval of the contamination event (i.e., CO_2 flow rate ≈ 0). Panel (c): vertical profiles of temperature (light blue) and RH (dark blue) in the instrument's enclosure, measured by the MS8607 sensor. Panel (d): vertical profile of H_2O mixing ratio in the instrument's enclosure (H_2O_{Box}) derived from the MS8607 measurements (blue line), overlaid with the estimates of H_2O_{Box} from the fit coefficient *a* of the 5 contaminated intervals in the stratosphere (red dots), calculated according to Eq. S3 (see text for details).